AGU PUBLICATIONS

JGR

Journal of Geophysical Research: Atmospheres

RESEARCH ARTICLE
10.1002/2014JD021842

Key Points:
- A total of 103 out of 827 NBEs initiated lightning flashes. All are positive NBEs
- Such NBEs are mostly lower than 10 km while other NBEs higher than 10 km
- Characteristics of discharges following NBEs depend on NBE heights

Correspondence to:
T. Wu,
wu.ting@comf5.comm.eng.osaka-u.ac.jp

Citation:
Wu, T., S. Yoshida, T. Ushio, Z. Kawasaki, and D. Wang (2014), Lightning-initiator type of narrow bipolar events and their subsequent pulse trains, *J. Geophys. Res. Atmos.*, *119*, 7425–7438, doi:10.1002/2014JD021842.

Received 1 APR 2014
Accepted 4 JUN 2014
Accepted article online 10 JUN 2014
Published online 30 JUN 2014

Lightning-initiator type of narrow bipolar events and their subsequent pulse trains

Ting Wu[1], Satoru Yoshida[2], Tomoo Ushio[1], Zen Kawasaki[1], and Daohong Wang[3]

[1]Division of Electrical, Electronic and Information Engineering, Graduate School of Engineering, Osaka University, Osaka, Japan, [2]Meteorological Research Institute, Ibaraki, Japan, [3]Department of Electrical, Electronic and Computer Engineering, Gifu University, Gifu, Japan

Abstract Previous observations show that some narrow bipolar events (NBEs) can initiate intracloud discharges, but the role of NBE as lightning initiation is still unclear. During the summer of 2013, 827 NBEs were detected with a 3-D LF lightning location system in Osaka, Japan. Out of 638 positive NBEs, 103 occurred as the initial events of lightning flashes. These initiator-type NBEs, called "INBEs" in this paper, are always followed by positive pulse trains whose locations show upward propagations probably from the main negative charge region to the upper positive charge region. Most of INBEs develop into intracloud flashes. Only two INBEs develop into positive ground flashes and five INBEs develop into negative ground flashes. Pulse widths and peak amplitudes of electric field change waveforms of INBEs are almost the same as those of normal NBEs. A major difference is that INBEs have much lower discharge heights. Most of INBEs are lower than 10 km while normal NBEs are mainly higher than 10 km. Characteristics of positive pulse trains following INBEs are closely related with discharge heights of INBEs. Higher INBEs are usually followed by weaker, fewer, and less frequent positive pulses with slower upward propagations. As the height increases to above 10 km, NBEs are usually no longer followed by such positive pulses.

1. Introduction

As a special type of intracloud discharge (IC), narrow bipolar events (NBEs) have been attracting wide attentions in recent years. Characteristics of NBEs that distinguish them from regular ICs include narrow and bipolar electric field change (E-change) waveforms [e.g., *Smith et al.*, 1999], very intense VHF (very high frequency) radiation [*Le Vine*, 1980; *Smith et al.*, 1999; *Jacobson*, 2003], deficiency of optical radiation [*Light and Jacobson*, 2002; *Jacobson et al.*, 2013], large discharge height [*Smith et al.*, 2004; *Wu et al.*, 2012], and short channel length [*Nag and Rakov,* 2010; *Liu et al.*, 2012]. NBEs are found to be statistically correlated with convective strength of thunderstorms [*Jacobson and Heavner*, 2005; *Wiens et al.*, 2008]. Negative NBEs have an especially strong correlation with the deepest convections [*Wu et al.*, 2013]. These features make NBE a useful proxy for convective activities.

NBEs are also called compact intracloud discharges because of short channel lengths [*Nag et al.,* 2010; *Liu et al.,* 2012]. In this paper, we will use the name of NBE because only E-change data, in which NBEs are characterized by narrow and bipolar pulses, are used for this study. Identification of NBEs will be further discussed in next section.

NBEs have long been thought to be temporally isolated with other lightning discharges. *Le Vine* [1980] and *Willett et al.* [1989] noticed that NBEs had no apparent association with any other lightning process. *Smith et al.* [1999] concluded that NBEs produced in three thunderstorms were temporally isolated on a time scale of several seconds. More recent studies, however, found that at least some of NBEs serve as the initial processes of regular ICs. *Rison et al.* [1999] reported LMA (Lightning Mapping Array) observations of 13 positive NBEs that were all followed by ICs within 10 ms. *Thomas et al.* [2001] also reported some similar results with LMA observation. *Smith et al.* [2002], based on thousands of NBEs recorded by Los Alamos Sferic Array, stated that it was neither unusual nor common to see intracloud activities following NBEs. *Nag et al.* [2010], based on wideband electric fields, narrowband VHF radiation signals and location information reported by National Lightning Detection Network [*Cummins et al.,* 1998], reported that 5 out of 157 positive NBEs preceded ICs by 5.3–67 ms and another three NBEs preceded cloud-to-ground flashes (CGs) by 72–233 ms. *Wu et al.* [2011] made a statistical analysis on the temporal characteristics of NBE and found

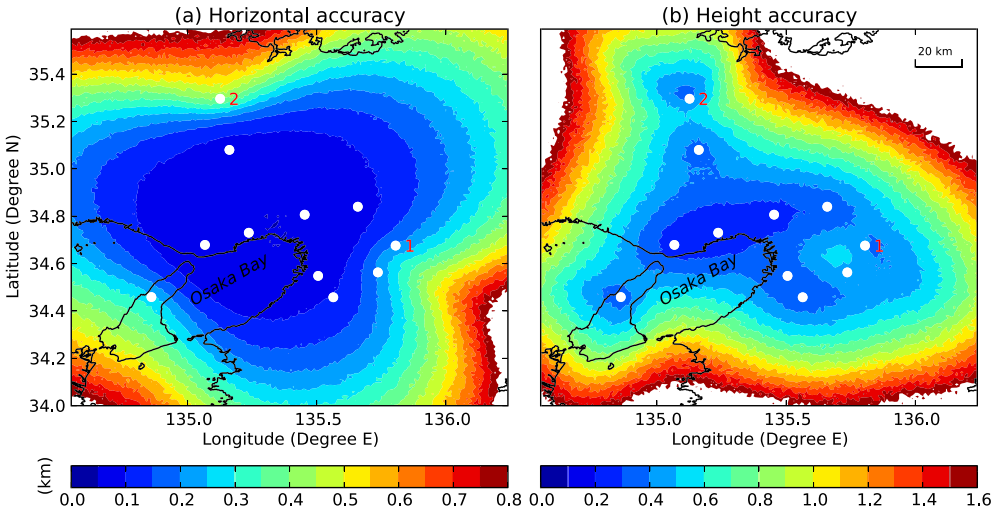

Figure 1. Simulation results of location accuracy of BOLT. Source height is 5 km. White points represent stations of BOLT. Sites labeled 1 and 2 are used in section 3.2.

that 11.7% of positive NBEs preceded while only 1.6% followed other discharge processes within 10 ms. The corresponding percentages for negative NBEs were 4.4% and 1.6%. These studies indicate that NBEs, especially positive ones, can occur as the initial events of lightning flashes. However, it is still unclear what kind of NBEs can initiate lightning discharges and under what conditions are such NBEs produced.

On the wideband E-change signal, lightning flashes typically start with a train of relatively large pulses lasting for several milliseconds [e.g., *Rakov,* 2006]. These pulses are called preliminary breakdown pulses (PBPs) or initial breakdown pulses. The initial polarities of PBPs are usually positive (physics sign convention) in ICs and negative in negative CGs. Based on observation data in four regions with different latitudes, *Marshall et al.* [2014] concluded that all negative CGs probably begin with PBPs. In another study, *Marshall et al.* [2013] presented location results of PBPs of several ICs. They reported that no NBEs were observed at the beginning of ICs. The current study, in contrast, will focus on NBEs that are the first events in lightning flashes.

In this paper, we will report observations of 827 NBEs including 103 NBEs as the beginning of lightning flashes with a three-dimensional (3-D) low-frequency (LF) lightning locating system during the summer of 2013. Various characteristics of NBEs as initiation processes will be analyzed and compared with those of normal NBEs. Characteristics of pulse trains following NBEs are closely related with NBE heights. Such relationship will be investigated.

2. Experiment and Data

Lightning discharges are detected and located with a LF lightning locating system called BOLT (Broadband Observation network for Lightning and Thunderstorms). It comprises 11 stations in Osaka region of Japan since June of 2013. Stations of BOLT are shown as white points in Figure 1, covering an area of about $90 \times 90\ km^2$.

Each station of BOLT is equipped with a fast antenna with a time constant of 200 μs and frequency range of 500 Hz to 500 kHz. E-change signals produced by lightning discharges are digitized at 4 MS/s sampling rate and in 16 bit resolution. Triggering time of each record is provided by a GPS receiver with a timing accuracy of 50 ns.

The record length is set to 200 ms with a 100 ms pretrigger. The upgraded recording system can be triggered continuously without any dead time. This allows detailed analysis of lightning discharges lasting a long time. In section 3.1, we will show E-change waveforms and 3-D location results with durations longer than 200 ms.

A simulation similar to that employed by *Bitzer et al.* [2013] is performed to estimate location accuracy of BOLT. A point discharge is assumed at each grid point with $0.01° \times 0.01°$ spacing within the range of Figure 1.

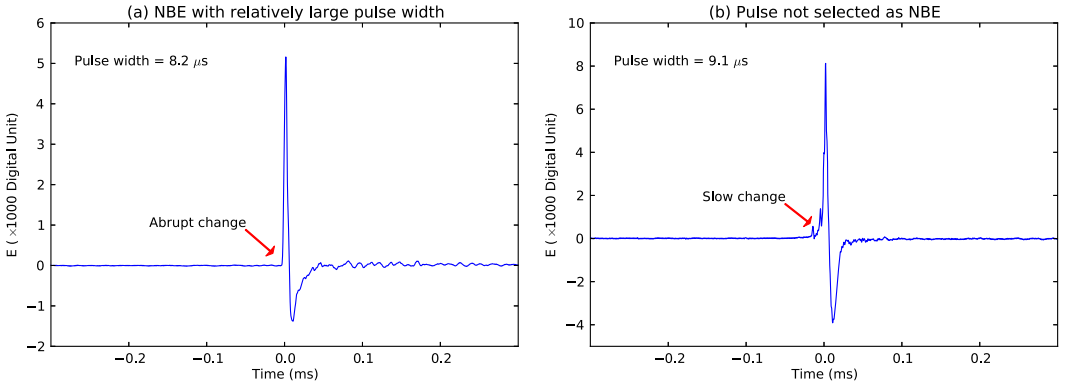

Figure 2. Pulses with similar waveforms and pulse widths. (a) Selected as NBE. (b) Not selected as NBE.

A random error from a normal distribution with a mean of 0 μs and a variance of 0.25 μs^2 is added to the arrival time at every station, and 3-D location of the source is calculated with the error-included arrival time and compared with the assumed location of the source. At each grid point, 1000 computations are performed and the average result is used. Figure 1 shows simulation results with a source of 5 km altitude.

In this study, only NBEs located in the area with a height accuracy of better than 1 km and a horizontal accuracy of better than 0.6 km are analyzed. Most of NBEs analyzed in this study are higher than 5 km, so they should have height accuracies better than that indicated in Figure 1b [*Bitzer et al.*, 2013; *Karunarathne et al.*, 2013].

NBEs are identified by E-change waveforms. Two criteria based on pulse width and signal-to-noise ratio (SNR) to automatically identify NBEs are widely used in previous studies [*Smith et al.,* 2002; *Hamlin et al.,* 2007; *Wu et al.,* 2011]. For example, *Hamlin et al.* [2007] identified waveforms with pulse width of smaller than 10 μs and SNR value of larger than 200 as NBEs. These values can be different in different studies, but the principles are the same, that is, pulse width should be small enough to ensure that the pulse is narrow, and SNR value should be large enough to ensure that the pulse is temporally isolated. The current study, however, focuses on NBEs initiating lightning flashes, which are inherently not isolated and thus have small SNR values. Therefore, we first automatically identify possible NBEs with quite loose criteria: pulse width of smaller than 12 μs and SNR of larger than 150. These criteria can effectively exclude return strokes and most of regular intracloud processes. Then NBEs are manually selected from these automatically identified records. In this step, only pulses with an abrupt change at the onset of the pulse are selected as NBEs. This feature is illustrated in Figure 2, which shows two pulses with similar waveforms and pulse widths. The second one is not selected as a NBE because it showed quite slow change at the rising portion. We believe such "abrupt change" feature is essential for NBEs. Because this study deals with NBEs at the very beginning of lightning flashes, this feature can also ensure that our selected NBEs are not pulses associated with normal initial breakdown processes.

NBEs produced from 4 July to 2 September of 2013 are analyzed. There are 638 positive NBEs and 189 negative NBEs. Among the positive NBEs, 103 occurred as the very first events of lightning flashes. No negative NBEs were found to have such behavior. For clarity, positive NBEs initiating lightning flashes will be indicated as "INBE" in the rest of this paper while normal positive NBEs will be indicated as "PNBE" and all negative NBEs will be indicated as "NNBE". So in this study, we have two types of "positive NBEs," including 103 INBEs and 535 PNBEs. Differences among INBE, PNBE, and NNBE will be investigated in this paper.

Physics sign convention is used in this paper, thus positive NBE could correspond to the discharge between lower negative charge and upper positive charge.

3. Results

3.1. INBEs and Processes Following Them

INBEs occur as the very first event of a lightning flash. They are followed by various discharge processes lasting for at least tens of milliseconds. One common feature of INBEs is that they are all followed directly by positive pulse trains. These positive pulse trains typically start within 10 ms of INBE and last for several to tens

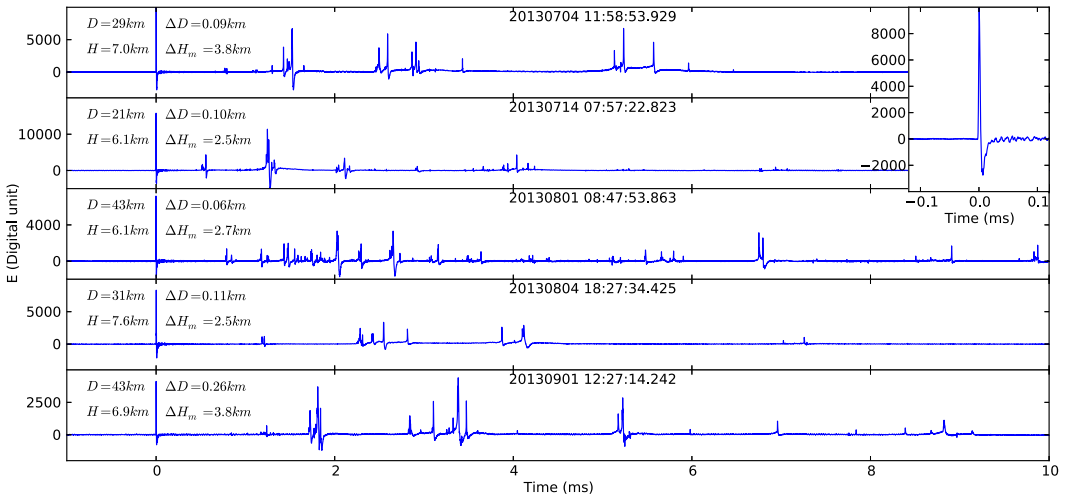

Figure 3. Electric field change waveforms of five typical INBEs and subsequent positive pulse trains. *D* is horizontal distance from INBE to observation station. *H* is discharge height of the INBE. $\triangle D$ is horizontal distance from the INBE to the first subsequent pulse. $\triangle H_m$ is height difference between the highest pulse within 10 ms after the INBE and the INBE. The inset shows an expanded waveform of the INBE in the first panel.

of milliseconds. Figure 3 shows five examples of E-change waveforms of INBEs and subsequent positive pulses within 10 ms. We can see that all the pulses following INBEs are of positive polarity, the same as INBE. Waveforms of these pulses are quite different from that of INBE. One essential difference is that they lack the "abrupt change" feature as illustrated in Figure 2.

Our LF lightning location system BOLT is capable of locating lightning discharges in three dimensions. Next we will present 3-D location results of INBEs and their subsequent positive pulses. Two examples are shown in Figure 4. Figure 4a shows a 5 ms record on 4 July 2013. The E-change waveform (bottom right panel) is similar to examples in Figure 3. The flash started with an INBE at an altitude of 6.4 km (top right panel). Locations of subsequent positive pulses showed clear upward propagation. The discharges progressed to the highest altitude (9.1 km) at 3.7 ms. The average speed of upward propagation was 7.3×10^5 m/s. In the plan view (left panel), it seems that the discharges first developed in one channel for about 3 ms and then it branched into two directions. The scale of horizontal propagation is about 1.5 km.

As another example Figure 4b shows a 6 ms record on 1 September 2013. Its E-change waveform is also similar to previous examples. This flash started with an INBE at an altitude of 6.2 km and propagated upward for 5.3 ms to the highest altitude of 8.9 km. The average speed of upward propagation was 5.1×10^5 m/s. In the plan view, the discharges seemed to progress in two opposite directions, and each direction of progression later branched into two directions. However, the scale of horizontal propagation is quite small, with the farthest location point only about 1 km from the INBE.

From these two examples, we can see one distinguishing feature of INBEs, that is, locations of positive pulses following them always show clear upward propagations. For the cases shown in Figure 3, all their upward propagation heights are estimated and are indicated by the values of $\triangle H_m$. As seen from these values, discharges following INBEs in Figure 3 propagated upward for 2.5 to 3.8 km.

After this "upward propagation" stage, pulses start to change polarity and their source heights usually decrease. It seems that the discharges can develop into any type of lightning flashes and no common characteristics can be identified. Most of INBEs ended in intracloud discharge processes. Only two INBEs developed into positive CGs and five INBEs developed into negative CGs. Two positive CGs were both single-stroke flashes while five negative CGs include one two-stroke flash and one four-stroke flash. Time differences and horizontal distances between INBE and the first return stroke ranged from 110.5 to 1076.0 ms and from 0.9 to 13.7 km, respectively. As an example, Figure 5 shows location results of a positive CG and a negative CG initiated by INBEs.

Figure 5a shows a positive CG initiated by an INBE on 4 July 2013. INBE was the very first event in this flash. After about 257 ms, a positive return stroke occurred. Discharges within about 4 ms of the INBE showed

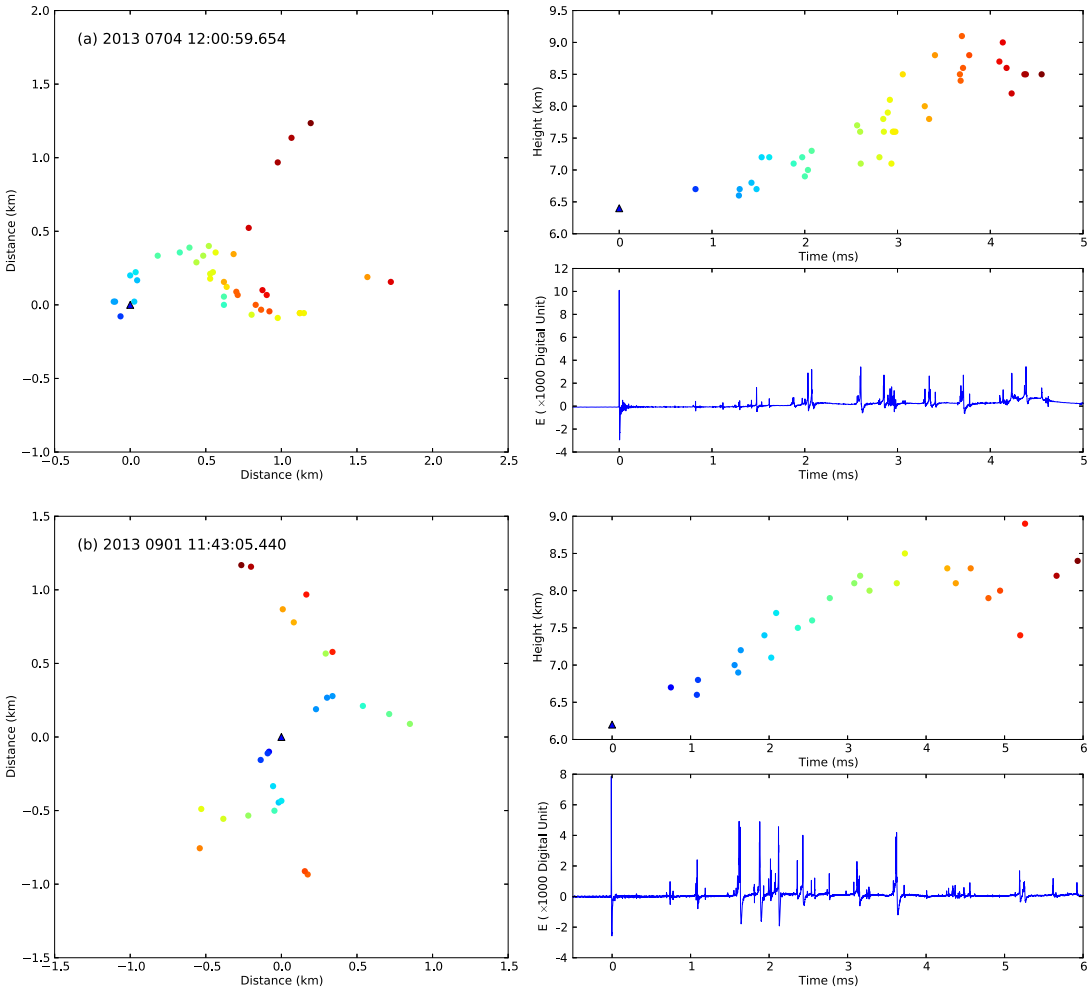

Figure 4. (a and b) Two examples of 3-D locations of INBEs and subsequent positive pulses.

predominantly upward propagation similar to the cases in Figure 4. The average speed of upward propagation was 9.5×10^5 m/s. After the upward propagation stage, source heights gradually decreased back to the height of INBE. No clear discharge processes occurred during the following 150 ms. At about 210 ms, some intracloud discharge processes started, but from the plan view, these processes started at about 10 km away from the INBE and propagated further away with several branches. Stepped leaders and a positive return stroke occurred following these intracloud processes at locations much closer to the INBE. It seems that the return stroke was associated with the INBE and its subsequent upward propagation discharges.

Figure 5b shows a negative CG initiated by an INBE on 1 September 2013. This flash first showed relatively rapid upward propagation within about 16 ms with an average speed of 3.0×10^5 m/s. Before 100 ms, the flash kept propagating upward to an altitude of 12.9 km. Different from the previous case, this flash did not show downward propagation after the upward propagation stage. Instead, a new upward propagation process was initiated at a location close to the INBE (horizontal distance was 1.6 km). It propagated upward for about 25 ms and was followed by gradual downward propagation. Before about 400 ms, source heights stayed within about 6 to 9 km. After 400 ms, source heights were generally lower than 5 km. The negative return stroke occurred at 619.4 ms. However, no stepped leader signals could be identified before the return stroke. From the plan view, it can be seen that processes before about 250 ms (blue points) showed several clear branches. These processes corresponded to the initial two upward propagation stages and subsequent downward-propagation stage. Processes after them did not show clear channels in the plan view.

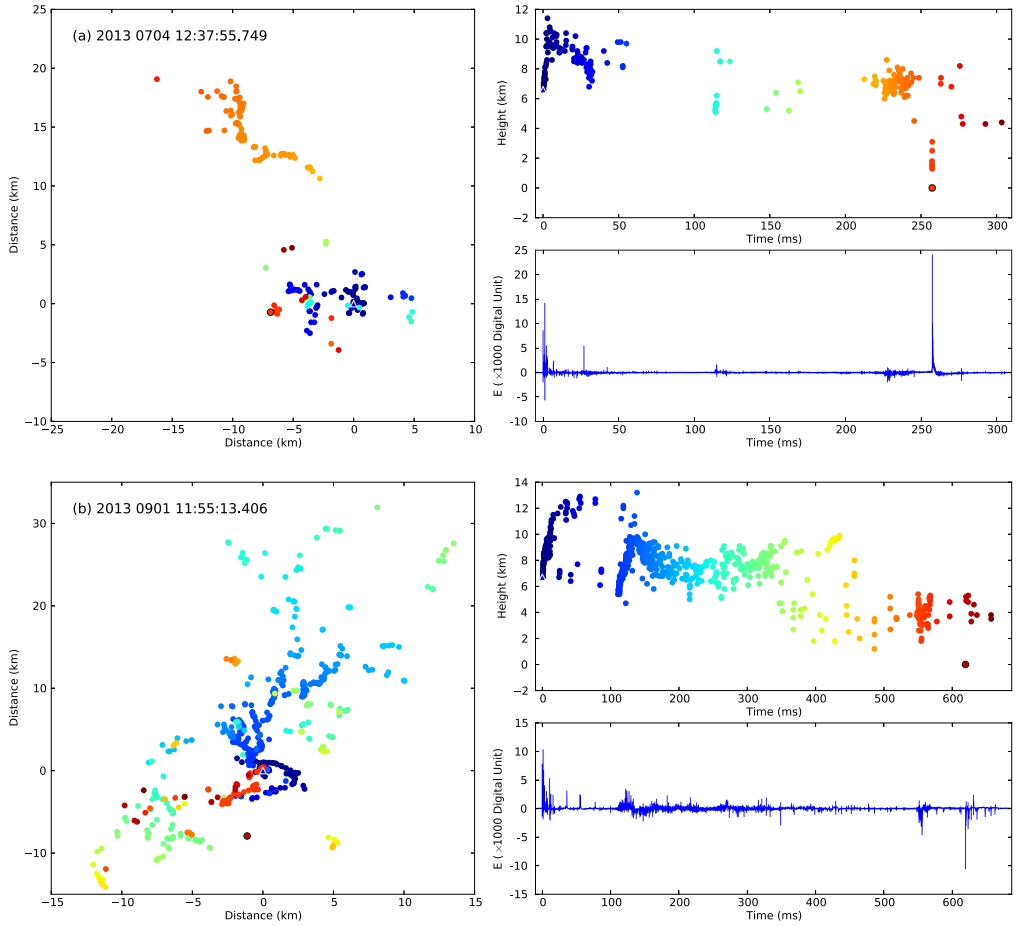

Figure 5. Examples of 3-D locations of (a) a positive CG and (b) a negative CG initiated by INBEs. INBEs are indicated as triangles and return strokes are indicated as black circles. There is only one return stroke in both cases.

From these examples, it is clear that INBEs are followed by discharge processes propagating upward for several kilometers, and these upward propagating processes produce positive pulse trains in E-change records. It is speculated that INBEs are produced at the upper boundary of the main negative charge region, and subsequent processes propagate upward to the upper positive charge region. INBE together with its subsequent upward propagating process seems to serve as the initiation process in a lightning flash. This is very similar to PBPs in ICs. Several recent studies reported source heights of PBPs in ICs located by networks of wideband E-change sensors [*Bitzer et al.,* 2013; *Karunarathne et al.,* 2013; *Marshall et al.,* 2013], which showed very similar upward propagations. *Marshall et al.* [2013] stated that PBPs of ICs were directly related with preliminary breakdown processes, which moved upward from the main negative charge to the upper positive charge. It seems that INBEs with subsequent positive pulse trains have the same behavior as PBPs of ICs. They may be a special type of PBPs with the first pulse produced by a NBE.

3.2. Comparison of INBEs and Normal NBEs

NBEs are generally thought to be temporally isolated. INBEs, however, have shown to be followed by positive pulses. So one obvious difference between INBEs and regular NBEs is that INBEs are never temporally isolated. However, why do some NBEs initiate lightning flashes (INBEs) while some do not (PNBEs and NNBEs)? They should have some essential differences. In this section, we will explore possible differences between INBEs and normal NBEs including PNBEs and NNBEs.

3.2.1. Pulse Width

First, pulse widths are compared for INBEs, PNBEs, and NNBEs. The pulse width is defined as the time from 10% peak amplitude at the rising part to zero crossing at the falling part. Here we only use NBEs at least 50 km

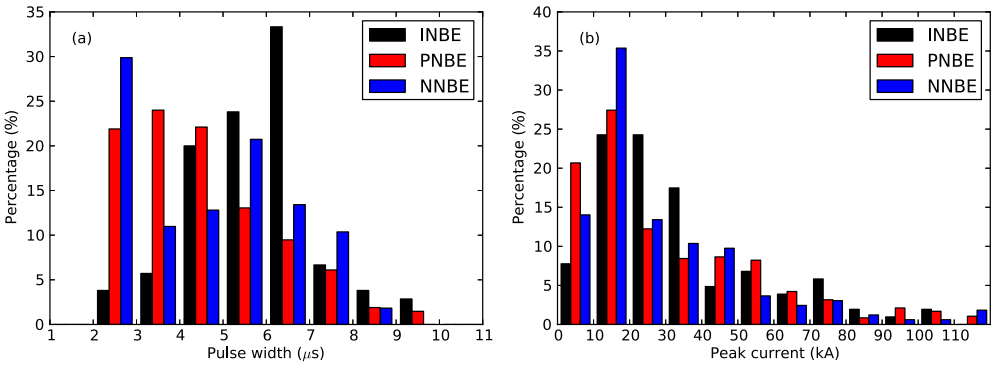

Figure 6. Distributions of (a) pulse width and (b) estimated peak current of INBEs, PNBEs, and NNBEs.

away from site 1 or site 2 as indicated in Figure 1, because waveforms produced by close events include static field component and may result in very different results of pulse width. For every NBE, if it is more than 50 km away from site 1, then waveform recorded at site 1 is used. If not, check whether it is more than 50 km away from site 2. If it is, waveform recorded at site 2 is used, and if not, this NBE is not included for this analysis. With this routine, all 103 INBEs, 474 of 535 PNBEs, and 164 of 189 NNBEs are selected for this analysis. Distributions of pulse width are shown in Figure 6a.

Distributions of pulse width for INBEs, PNBEs, and NNBEs show certain differences. Distribution for NNBEs is mainly from 2 to 6 μs and shows largest percentage from 2 to 3 μs. Distribution for PNBEs shows relatively large percentages from 2 to 5 μs. Distribution for INBEs shows very small percentages below 4 μs, and most of INBEs have pulse widths from 4 to 7 μs. The average values of pulse width for INBEs, PNBEs, and NNBEs are 5.8 μs, 4.5 μs, and 4.6 μs, respectively. It seems that INBEs have slightly larger pulse widths. However, pulse widths of three types of NBEs are distributed in almost the same range, from 2 to 10 μs, so the slight difference of pulse width between INBEs and other NBEs is not essential; it is not possible to tell whether one NBE is INBE or not from its pulse width.

3.2.2. Peak Amplitude

In this section, peak amplitudes of E-changes produced by INBEs, PNBEs, and NNBEs are compared to investigate whether the radiation power of three types of NBEs at LF band has any difference. The same data set as the analysis of pulse width is used. All NBEs in the analysis are at least 50 km away from site 1 or site 2, so peak amplitudes of E-changes can be normalized to 100 km using the simple 1/R relationship. However, E-changes recorded at site 1 and site 2 may have different gains, so they cannot be compared directly. Here we use the same method as in *Wu et al.* [2014] to convert the normalized E-change amplitudes to peak currents, and peak currents estimated from site 1 and site 2 can be compared with each other. *Wu et al.* [2014] compared normalized E-change amplitudes recorded at site 1 and peak currents reported by lightning location system of Japan for hundreds of return strokes and found a linear relationship between normalized E-change amplitudes and peak currents. The linear relationship can be written as

$$I_p = \alpha E_p$$

where I_p is the peak current in kiloampere, E_p is the normalized E-change amplitude in digital unit, and α is the coefficient of proportionality. For site 1, $\alpha = 0.0113$ [*Wu et al.,* 2014]. The value of α for site 2 can be worked out in exactly the same way, and the value is 0.0147. With this relationship, normalized E-change amplitudes recorded at site 1 and site 2 are all converted to peak currents, and peak currents of INBEs, PNBEs, and NNBEs can be compared. Note that these peak currents are probably different from the true current values of NBEs. The main purpose of the conversion is to make the records of site 1 and site 2 comparable.

Distributions of estimated peak currents of INBEs, PNBEs, and NNBEs are shown in Figure 6b. Three types of NBEs have very similar distributions with peak distributions around 20 kA. Average values are 33.1 kA, 32.3 kA, and 34.4 kA, respectively, for INBEs, PNBEs, and NNBEs, also very similar with each other. Therefore, three types of NBEs produce very similar E-field change magnitudes.

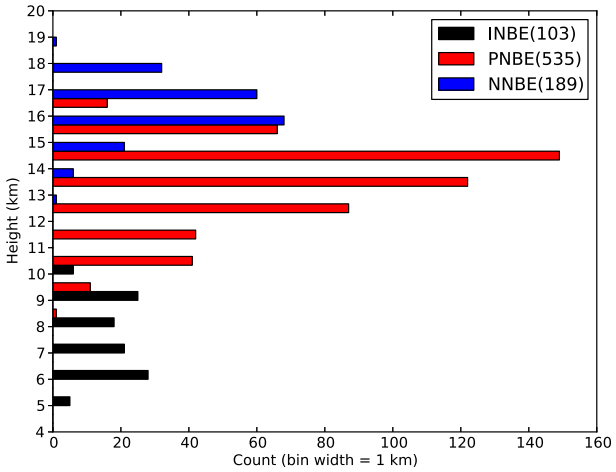

Figure 7. Discharge height distributions of different types of NBEs. Numbers in the parentheses are sample sizes.

3.2.3. Discharge Height

Discharge heights of INBEs, PNBEs, and NNBEs are compared in this section. Height of lightning discharge is an essential property because it determines the location of the discharge in a thundercloud and thus the meteorological context in which the discharge is produced. It is now well known that positive NBEs are generally lower than negative NBEs. Positive and negative NBEs, respectively, are inferred to be produced below and above the upper positive charge region [*Smith et al.,* 2004; *Wu et al.,* 2012]. In this study, we also find that positive NBEs are generally lower than negative NBEs. A surprising result, however, is that most INBEs are lower than PNBEs as shown in Figure 7.

The average heights for NNBEs, PNBEs, and INBEs are 15.9 km, 13.4 km, and 7.9 km, respectively. In Figure 7, NNBEs are generally higher than PNBEs with some overlaps around 16 km. This result is similar to previous studies. On the other hand, although INBEs and PNBEs are both positive polarity NBEs, most INBEs are lower than PNBEs. It seems that 10 km altitude is an appropriate dividing altitude between INBEs and PNBEs. For INBEs, 97 of 103 (94.2%) are lower than 10 km while for PNBEs, 523 of 535 (97.8%) are higher than 10 km. Therefore, positive NBEs higher than 10 km are probably PNBEs while those lower than 10 km are probably INBEs. In other words, NBEs lower than 10 km are probably followed by positive pulse trains.

From the above results we can see that pulse widths of INBEs and PNBEs are in the same range, and E-change magnitudes produced by them are almost the same, so from the E-change pulse waveform, it is not possible to tell whether it is produced by an INBE or a PNBE. However, they can be simply differentiated with their discharge heights: NBEs lower than 10 km are probably INBEs, followed by positive pulse trains with upward propagations. This result is consistent with LMA observations of an INBE between 8 and 9 km altitude [*Rison et al.,* 1999] and another one between 6 and 7 km altitude [*Thomas et al.,* 2001].

3.3. Characteristics of Discharge Processes Following INBEs

Section 3.1 demonstrated that INBEs are followed by positive pulses whose locations show clear upward propagations, and section 3.2 demonstrated that discharge heights of INBEs are mostly lower than 10 km while regular positive NBEs are mostly higher than 10 km. Interestingly, these two conclusions have certain connections with each other. It is found that characteristics of positive pulses following INBEs are closely related with discharge heights of INBEs, which will be analyzed in this section.

3.3.1. Positive Pulse Trains After INBEs

Figure 8 shows scatterplots of some properties of positive pulse trains following INBEs versus source heights of INBEs. Pulses in a pulse train include all pulses after an INBE until a pulse with clear negative initial polarity occurs.

Figures 8a–8c are about amplitudes of pulses in each train with (a) the amplitude of the first pulse, (b) the amplitude of the largest pulse, and (c) the average amplitude of all pulses in a pulse train relative to the amplitude of the corresponding INBE. As seen in these figures, all the three amplitude ratios decrease with increasing height of INBE. They indicate that as the height of INBE increases, pulses following it become weaker.

Figure 8d shows the time difference between the first pulse in a pulse train and INBE. As the height of INBE increases, the time difference gets larger, indicating that it takes longer time for pulse trains of higher INBEs to start. Figure 8e shows the duration of the pulse train. As the height of INBE increases, pulse train duration also gets larger. However, as Figure 8f shows, as the height of INBE increases, pulse number in a train gets

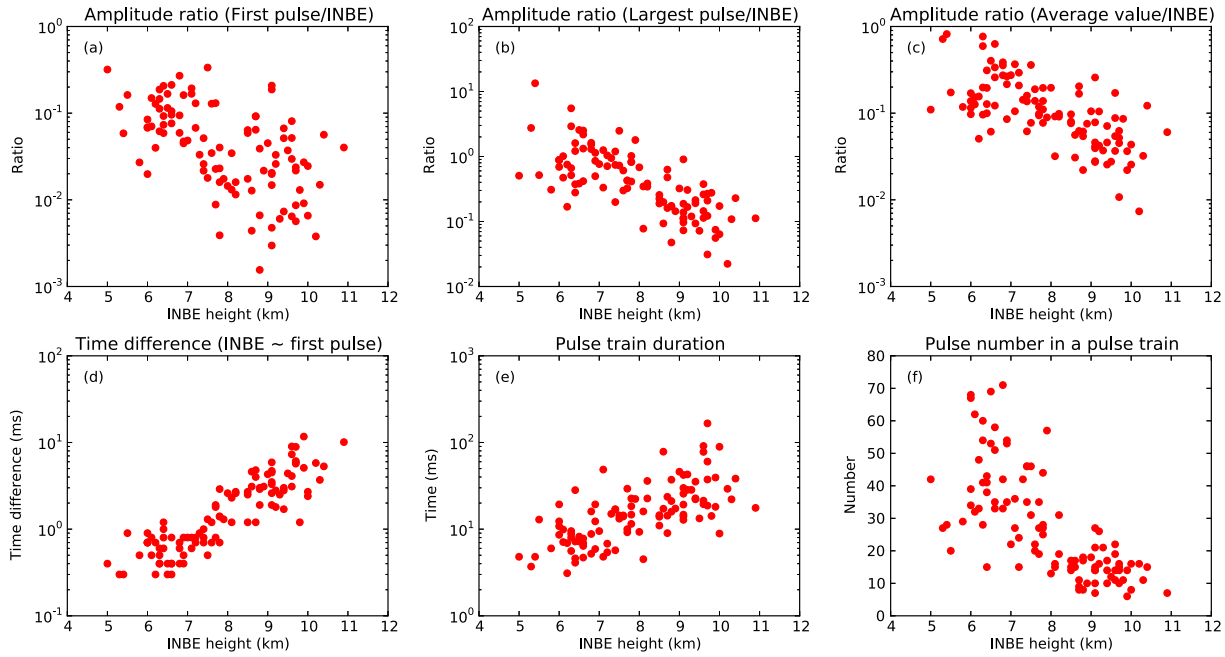

Figure 8. Scatterplots of some properties of the positive pulse trains following INBEs versus discharge heights of INBEs. (a) Ratio of amplitude of the first pulse in the train to that of INBE. (b) Ratio of the amplitude of the largest pulse in the train to that of INBE. (c) Ratio of average amplitude of all pulses in the train to INBE amplitude. (d) Time difference between the first pulse in the train and INBE. (e) Duration of the pulse train. (f) Number of pulses in the pulse train.

smaller. These results indicate that as the height of INBE increases, its subsequent pulse train includes fewer pulses, but the time differences between pulses get larger and the duration of the pulse train gets longer.

The above results indicate that as the height of INBE increases, pulses following it become weaker and less frequent. It seems that certain conditions at higher altitudes make pulses following INBEs more difficult to occur.

From Figure 8 we can also see some other characteristics. The amplitude of the first pulse in a train is always smaller, most of the time much smaller, than that of INBE (Figure 8a). This is very different from PBPs, in which the first pulse is usually much smaller than other pulses (see examples in *Gomes et al.* [1998] and *Ushio et al.* [1998]). However, the amplitude of the largest pulse in a train can be larger than that of INBE (Figure 8b). The case with the largest ratio in this study is shown in Figure 9a. In this case, the amplitude of the largest pulse (saturated) in the pulse train is about 14 times of that of the INBE.

The time difference between INBE and the first pulse in a train is at least 0.3 ms and can be as large as 10 ms (Figure 8d). So if the recording length is set to be too small (for example, several milliseconds), INBEs can be misidentified as normal positive NBEs.

3.3.2. Characteristics of Upward Propagations

As demonstrated in section 3.1, locations of positive pulses following INBEs show clear upward propagations. Characteristics of upward propagations are also related with heights of INBEs. Figure 10 is a rough illustration of upward propagations of all INBEs shown in four height ranges. Each line in the figure represents one INBE with its subsequent pulse train. The left end of each line represents time and height of INBE and the right end represents time and height of the highest pulse in its subsequent pulse train, so the slope of each line can be seen as the overall speed of upward propagation. A clear trend is that lines of lower INBEs show steeper slopes, indicating lower INBEs are followed by more rapid upward propagations.

In order to analyze this feature in detail, Figure 11 shows scatterplots of some properties of the upward propagation versus INBE height. Figures 11a and 11b show upward propagation height and duration, from which the average speed can be calculated and is shown in Figure 11c. Height and duration of upward propagation are height difference and time difference, respectively, between INBE and the positive pulse of largest height in each pulse train, the same as those in Figure 10. From Figure 11, we can see that upward

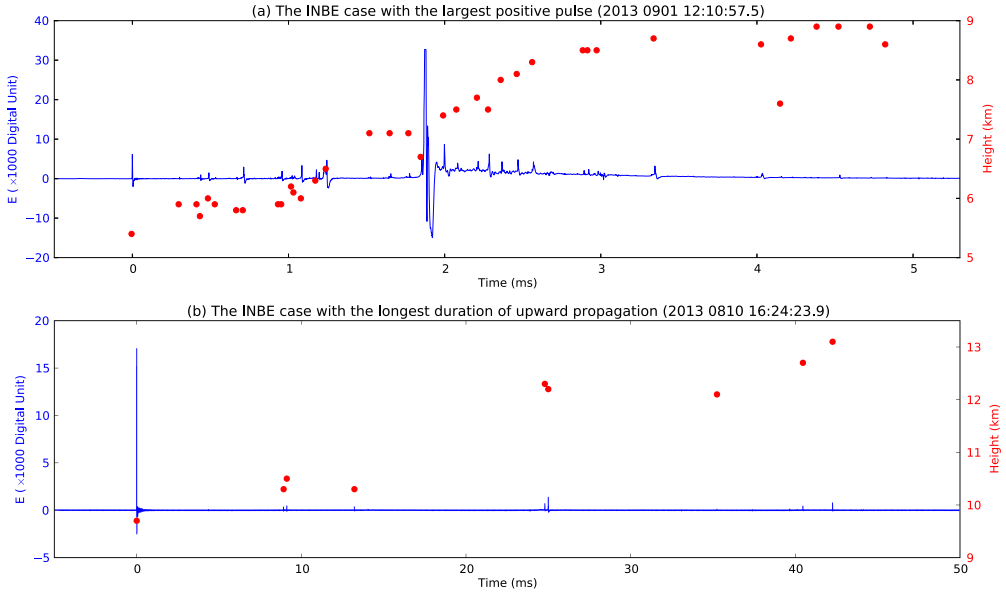

Figure 9. (a and b) Two special cases of INBEs. Red points indicate heights of corresponding pulses.

propagation height shows a decreasing tendency with increasing INBE height, and upward propagation duration generally increases with increasing INBE height. As a result, upward propagation speed decreases with increasing INBE height.

The speed values shown in Figure 11 are average values in vertical direction. The actual speed values should be larger because the propagations also have horizontal components as shown in Figures 4 and 5.

Speed values in this study are generally larger than estimations of initial leader speeds in previous studies. For example, *Shao and Krehbiel* [1996] reported that preliminary breakdown propagated upward at a speed of 1.5 to 3×10^5 m/s observed by a 2-D interferometer. *Behnke et al.* [2005] reported initial leaders in ICs starting at a median speed of about 1.6×10^5 m/s with LMA observation. In our study, speeds of upward propagations following INBEs have an average value of 3.3×10^5 m/s and a median value of 2.9×10^5 m/s. Lower INBEs are usually followed by rapid upward propagations with speeds generally larger than those reported in previous studies. Four INBEs shown in Figures 4 and 5 are between 6 and 7 km high and are followed by upward

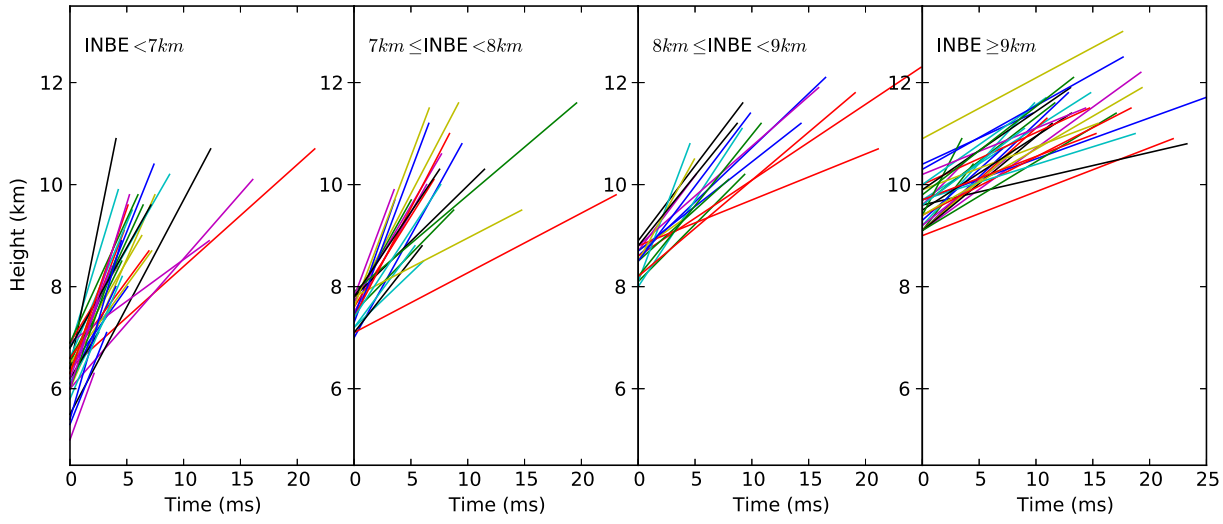

Figure 10. An illustration of upward propagations of discharges following INBEs. Each line represents one INBE with its subsequent pulses. Left end of each line represents INBE, and right end represents the pulse with the highest location. INBEs in different height ranges are in different panels. Line colors are randomly assigned.

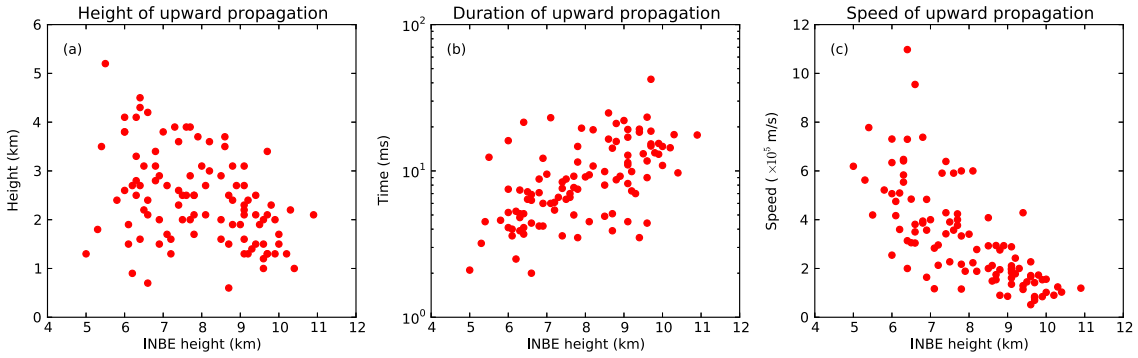

Figure 11. (a) Height, (b) duration, and (c) speed of upward propagation versus source height of INBE.

propagations with speeds of 7.3, 5.1, 9.5, and 3.0×10^5 m/s, respectively. On the other hand, higher INBEs, especially those higher than 9 km, are mostly followed by relatively slow upward propagations with speeds generally lower than 2.0×10^5 m/s. As an extreme example, Figure 9b shows an INBE followed by upward propagation with the longest duration. The discharge propagated upward for 3.4 km within 42.3 ms. The average speed was only 0.80×10^5 m/s. It is also interesting to note that positive pulses following the INBE in Figure 9b were extremely small compared with the INBE, as already demonstrated in Figures 8a–8c.

4. Discussions

4.1. Lightning Initiation by INBEs and by PBPs

INBEs with subsequent pulse trains are very similar to PBPs of positive initial polarity. Both of them typically occur before ICs. Positive PBPs are also reported to develop into negative CG, forming a "hybrid flash" [*Bitzer et al.,* 2013], which is also similar to the case shown in Figure 5b. Positive PBPs are inferred to be related to initial leaders propagating upward and establish a conducting channel between the main negative and upper positive charge regions [*Marshall et al.,* 2013], and INBEs with subsequent positive pulses also appear to be related to such initial leaders (section 3.1).

An apparent difference, however, is that the first pulse in PBPs does not have any discernable special features (examples can be seen in *Karunarathne et al.* [2013], *Marshall et al.* [2013] and references therein). It is usually relatively small and closely followed by subsequent pulses. On the contrary, INBE is usually much larger than subsequent positive pulses (Figures 8a–8c) and there is some quiet time between INBE and the onset of positive pulses (Figure 8d).

Speed of upward propagation may be another difference. Upward propagations following INBEs are somehow faster than those observed for preliminary breakdowns (section 3.3.2). However, observations of preliminary breakdowns with reliable location information are still very limited so detailed comparison of propagation speed is so far not possible.

If we assume positive PBPs have the same behavior as INBEs with subsequent positive pulses, there are some interesting questions to consider. First, characteristics of positive pulses following INBEs change with discharge heights of INBEs (section 3.3). Do characteristics of PBPs change with the discharge heights of the first pulses of PBPs? Second, most of INBEs are lower than 10 km and NBEs higher than 10 km are usually not followed by positive pulse trains. Are PBPs also only able to start at an altitude generally lower than 10 km? These questions may be essential for understanding lightning initiation mechanisms. We will investigate these questions in our future studies by analyzing 3-D location results of large number of PBPs.

4.2. Relationship Between Different Types of NBEs

INBEs, PNBEs, and NNBEs occur in different altitude ranges as shown in Figure 7. An expected result is that they correspond to different thunderstorms or different stages in a thunderstorm. Table 1 lists number of different types of NBEs in each thunderstorm during the summer of 2013. Three thunderstorms producing significant number of INBEs produced no NNBE while thunderstorms producing NNBEs produced at most

Table 1. Number of Different Types of NBEs in Each Thunderstorm[a]

Date	0704	0722	0727	0730	0731	0805	0807	0808	0823	0823	0901
INBE	16	0	10	0	1	1	1	0	0	0	49
PNBE	0	13	11	52	55	41	25	26	67	190	6
NNBE	0	4	0	1	26	49	0	14	25	62	0

[a]Only thunderstorms producing at least 10 NBEs of any type are included.

one INBE. NNBEs are considered to be produced in extremely vigorous thunderstorms [*Wu et al.,* 2013]. Thus, it seems likely that INBEs are only produced in relatively weak convections.

Table 1 also shows that thunderstorms producing primarily PNBEs usually produced few INBEs. However, two storm days (27 July and 1 September) did not exactly fit this statement. These two cases are shown in Figure 12.

Figure 12a shows time evolution of discharge heights of INBEs and PNBEs in the thunderstorm on 27 July. PNBEs were mainly produced at the later stage of the thunderstorm, and during the period of PNBE productions, no INBEs were produced. It seems PNBEs and INBEs were produced in different stages of the thunderstorm.

Figure 12b shows the case on 1 September. In this case, PNBEs were produced along with INBEs. During the period when PNBEs were produced, INBE rate and discharge heights were highest during the thunderstorm. This short period probably corresponds to the mature stage with relatively strong convection compared with other periods during this thunderstorm.

It is interesting to note that PNBEs in these two cases are relatively low, mainly around 10 km. From Figure 7 we can see discharge heights of PNBEs are mainly from 12 to 16 km. In fact, these high PNBEs were produced in thunderstorms without INBEs as listed in Table 1. Thunderstorms producing INBEs, on the other hand, either produced no PNBEs or a few relatively low PNBEs.

This result indicates a gradual transition from INBE to PNBE as discharge height increases. Such a gradual transition can also be seen in Figures 8 and 11. NBEs with low discharge heights are followed by positive pulse trains, and these NBEs are INBEs. Properties of positive pulse trains following INBEs are closely related with heights of INBEs. As the height of INBE increases, pulses following it become smaller and less frequent, and they last longer time and propagate upward with slower speed. As the height of NBE increases to above 10 km, it usually becomes normal NBE without pulses following it.

This transition is roughly illustrated in Figure 13. The general picture seems to be that as height of NBE increases, subsequent positive pulses become more difficult to occur, and when the height of NBE is higher than 10 km, almost no pulses can occur and the NBE changes from INBE to PNBE. Around 10 km, there is a transition stage, in which both INBEs and PNBEs are possible to occur. The thunderstorm case in Figure 12b illustrates this point. Away from 10 km, either INBEs or PNBEs can occur.

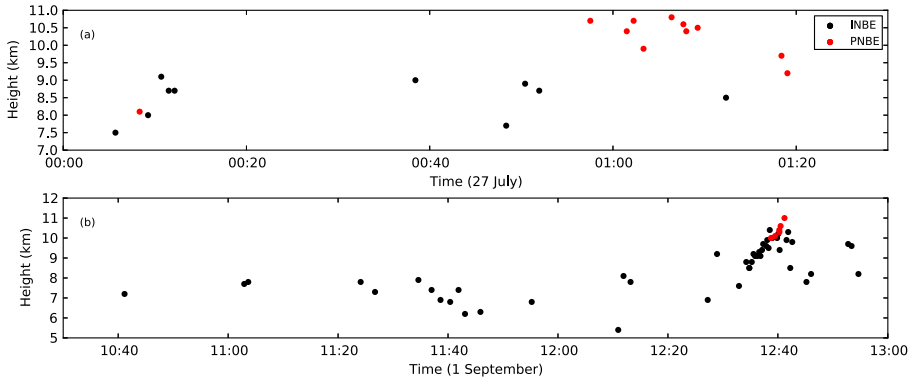

Figure 12. Time evolutions of discharge heights of INBEs and PNBEs in two thunderstorms.

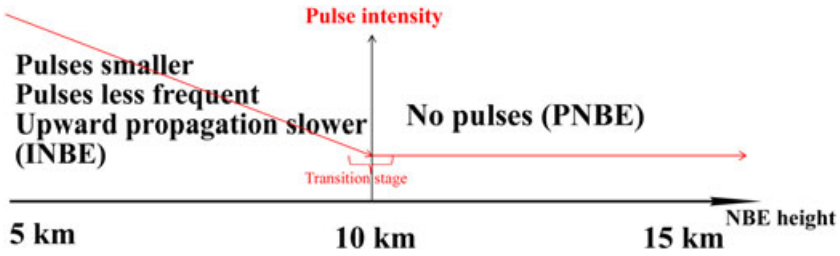

Figure 13. Illustration of the transition from INBE to PNBE.

As evident in Figure 4, the positive pulses following INBEs are produced by upward propagating negative leaders. We speculate that at higher altitudes, the electric field required to sustain continuous propagations of these leaders is relatively weak. When the leader propagates upward, it may encounter fewer and smaller positive charges and thus produce fewer and weaker E-change pulses. This may explain why higher INBEs are generally followed by fewer, weaker, and less frequent positive pulses.

One further question concerning INBEs and PNBEs is whether they are produced at the same region in thunderclouds. Both of them are produced between the main negative and upper positive charge regions. As described previously in this paper, INBEs are inferred to be produced at the upper edge of the main negative charge region. The thunderstorm case in Figure 12b shows that a few relatively low PNBEs were produced in the same period and similar altitudes as some relatively high INBEs. These PNBEs appeared to be the same as INBEs, produced at the upper edge of the main negative charge region. However, it seems that the majority of PNBEs, mostly higher than 12 km and up to 16 km, are produced close to the lower edge of the upper positive charge region, because it is almost impossible for the main negative charge region to be lifted to this altitude. It is also possible that some relatively low PNBEs are actually INBEs. They are also followed by upward propagating negative leaders, but these leaders produce too weak E-change signals to be detected.

Detailed studies on thunderstorms producing different types of NBEs are needed to further explore their relationships. These studies will also be valuable for inferring thunderstorm characteristics from NBE types.

5. Conclusions

A total of 827 NBEs were observed during the summer of 2013. These NBEs were classified into 103 INBEs, 535 PNBEs, and 189 NNBEs. This paper investigated various characteristics of INBEs, which were the initial events of lightning flashes. All of INBEs are of positive polarity, the same as PNBEs.

INBEs are always followed by positive pulse trains, locations of which show predominantly upward propagations. It is speculated that INBEs are produced at the upper edge of the main negative charge region and are followed by negative leaders propagating upward to the upper positive charge layer. Most of INBEs developed into ICs. Only two INBEs developed into positive CGs and five INBEs developed into negative CGs.

Pulse widths and peak amplitudes of E-change fields produced by INBEs are very similar to those produced by PNBEs and NNBEs. However, discharge heights of three types of NBEs show very different distributions. Most of INBEs are below 10 km while most of PNBEs are above 10 km. NNBEs are generally higher than INBEs and PNBEs.

An interesting and somehow mysterious result is that characteristics of positive pulses following INBEs are closely related with heights of INBEs. As the height of an INBE increases, positive pulses following it become weaker, fewer, and less frequent. It appears that at higher altitudes, these positive pulses are more difficult to occur.

Upward propagation speeds are also related with INBE heights. Higher INBEs are generally followed by slower upward propagations. Speeds of upward propagations following INBEs higher than 9 km are mainly around 1×10^5 m/s while those of INBEs lower than 9 km are mainly in the range of 2 to 8×10^5 m/s.

It seems that as discharge height increases, NBEs gradually change from INBEs to PNBEs. Such a transition is currently not fully understood. Different types of NBEs are apparently associated with thunderstorms with

different convective strength. More detailed analysis on properties of thunderstorms producing different types of NBEs will be carried out.

Acknowledgments
The data for this paper were obtained during the summer campaign in 2013. Readers can request the data from the corresponding author. This work was supported by the Japanese Ministry of Education, Science, Sports and Culture, a Japanese Grant-in-Aid for Scientific Research. The authors thank the reviewers for valuable comments.

References

Behnke, S. A., R. J. Thomas, P. R. Krehbiel, and W. Rison (2005), Initial leader velocities during intracloud lightning: Possible evidence for a runaway breakdown effect, *J. Geophys. Res.*, *110*, D10207, doi:10.1029/2004JD005312.

Bitzer, P. M., H. J. Christian, M. Stewart, J. Burchfield, S. Podgorny, D. Corredor, J. Hall, E. Kuznetsov, and V. Franklin (2013), Characterization and applications of VLF/LF source locations from lightning using the Huntsville Alabama Marx Meter Array, *J. Geophys. Res. Atmos.*, *118*, 3120–3138, doi:10.1002/jgrd.50271.

Cummins, K. L., M. J. Murphy, E. A. Bardo, W. L. Hiscox, R. B. Pyle, and A. E. Pifer (1998), A combined TOA/MDF technology upgrade of the U.S. National Lightning Detection Network, *J. Geophys. Res.*, *103*(D8), 9035–9044, doi:10.1029/98JD00153.

Gomes, C., V. Cooray, and C. Jayaratne (1998), Comparison of preliminary breakdown pulses observed in Sweden and in Sri Lanka, *J. Atmos. Sol. Terr. Phys.*, *60*, 975–979.

Hamlin, T., T. E. Light, X. M. Shao, K. B. Eack, and J. D. Harlin (2007), Estimating lightning channel characteristics of positive narrow bipolar events using intrachannel current reflection signatures, *J. Geophys. Res.*, *112*, D14108, doi:10.1029/2007JD008471.

Jacobson, A. R. (2003), How do the strongest radio pulses from thunderstorms relate to lightning flashes?, *J. Geophys. Res.*, *108*(D24), 4778, doi:10.1029/2003JD003936.

Jacobson, A. R., and M. J. Heavner (2005), Comparison of narrow bipolar events with ordinary lightning as proxies for severe convection, *Mon. Weather Rev.*, *133*, 1144–1154, doi:10.1175/MWR2915.1.

Jacobson, A. R., T. E. L. Light, T. Hamlin, and R. Nemzek (2013), Joint radio and optical observations of the most radio-powerful intracloud lightning discharges, *Ann. Geophys.*, *31*, 563–580, doi:10.5194/angeo-31-563-2013.

Karunarathne, S., T. C. Marshall, M. Stolzenburg, N. Karunarathna, L. E. Vickers, T. A. Warner, and R. E. Orville (2013), Locating initial breakdown pulses using electric field change network, *J. Geophys. Res. Atmos.*, *118*, 7129–7141, doi:10.1002/jgrd.50441.

Le Vine, D. M. (1980), Sources of the strongest RF radiation from lightning, *J. Geophys. Res.*, *85*(C7), 4091–4095, doi:10.1029/JC085iC07p04091.

Light, T. E. L., and A. R. Jacobson (2002), Characteristics of impulsive VHF lightning signals observed by the FORTE satellite, *J. Geophys. Res.*, *107*(D24), 4756, doi:10.1029/2001JD001585.

Liu, H., W. Dong, T. Wu, D. Zheng, and Y. Zhang (2012), Observation of compact intracloud discharges using VHF broadband interferometers, *J. Geophys. Res.*, *117*, D01203, doi:10.1029/2011JD016185.

Marshall, T., M. Stolzenburg, S. Karunarathne, S. Cummer, G. Lu, H.-D. Betz, M. Briggs, V. Connaughton, and S. Xiong (2013), Initial breakdown pulses in intracloud lightning flashes and their relation to terrestrial gamma ray flashes, *J. Geophys. Res. Atmos.*, *118*, 10,907–10,925, doi:10.1002/jgrd.50866.

Marshall, T., W. Schulz, N. Karunarathna, S. Karunarathne, M. Stolzenburg, C. Vergeiner, and T. Warner (2014), On the percentage of lightning flashes that begin with initial breakdown pulses, *J. Geophys. Res. Atmos.*, *119*, 445–460, doi:10.1002/2013JD020854.

Nag, A., and V. A. Rakov (2010), Compact intracloud lightning discharges: 1. Mechanism of electromagnetic radiation and modeling, *J. Geophys. Res.*, *115*, D20102, doi:10.1029/2010JD014235.

Nag, A., V. A. Rakov, D. Tsalikis, and J. A. Cramer (2010), On phenomenology of compact intracloud lightning discharges, *J. Geophys. Res.*, *115*, D14115, doi:10.1029/2009JD012957.

Rakov, V. A. (2006), Initiation of lightning in thunderclouds, *Proc. SPIE Int. Soc. Opt. Eng.*, 5975, 597512.

Rison, W., R. J. Thomas, P. R. Krehbiel, T. Hamlin, and J. Harlin (1999), A GPS-based three-dimensional lightning mapping system: Initial observations in central New Mexico, *J. Geophys. Res.*, *26*(23), 3573–3576, doi:10.1029/1999GL010856.

Shao, X. M., and P. R. Krehbiel (1996), The spatial and temporal development of intracloud lightning, *J. Geophys. Res.*, *101*(D21), 26,641–26,668, doi:10.1029/96JD01803.

Smith, D. A., X. M. Shao, D. N. Holden, C. T. Rhodes, M. Brook, P. R. Krehbiel, M. Stanley, W. Rison, and R. J. Thomas (1999), A distinct class of isolated intracloud lightning discharges and their associated radio emissions, *J. Geophys. Res.*, *104*(D4), 4189–4212, doi:10.1029/1998JD200045.

Smith, D. A., K. B. Eack, J. Harlin, M. J. Heavner, A. R. Jacobson, R. S. Massey, X. M. Shao, and K. C. Wiens (2002), The Los Alamos Sferic Array: A research tool for lightning investigations, *J. Geophys. Res.*, *107*(D13), 4183, doi:10.1029/2001JD000502.

Smith, D. A., M. J. Heavner, A. R. Jacobson, X. M. Shao, R. S. Massey, R. J. Sheldon, and K. C. Wiens (2004), A method for determining intracloud lightning and ionospheric heights from VLF/LF electric field records, *Radio Sci.*, *39*, RS1010, doi:10.1029/2002RS002790.

Thomas, R. J., P. R. Krehbiel, W. Rison, T. Hamlin, J. Harlin, and D. Shown (2001), Observations of VHF source powers radiated by lightning, *J. Geophys. Res.*, *28*(1), 143–146, doi:10.1029/2000GL011464.

Ushio, T., Z.-I. Kawasaki, K. Matsu-ura, and D. Wang (1998), Electric fields of initial breakdown in positive ground flash, *J. Geophys. Res.*, *103*(D12), 14,135–14,139, doi:10.1029/97JD01975.

Wiens, K. C., T. Hamlin, J. Harlin, and D. M. Suszcynsky (2008), Relationships among Narrow Bipolar Events, "total" lightning, and radar-inferred convective strength in Great Plains thunderstorms, *J. Geophys. Res.*, *113*, D05201, doi:10.1029/2007JD009400.

Willett, J. C., J. C. Bailey, and E. P. Krider (1989), A class of unusual lightning electric field waveforms with very strong high-frequency radiation, *J. Geophys. Res.*, *94*(D13), 16,255–16,267, doi:10.1029/JD094iD13p16255.

Wu, T., W. Dong, Y. Zhang, and T. Wang (2011), Comparison of positive and negative compact intracloud discharges, *J. Geophys. Res.*, *116*, D03111, doi:10.1029/2010JD015233.

Wu, T., W. Dong, Y. Zhang, T. Funaki, S. Yoshida, T. Morimoto, T. Ushio, and Z. Kawasaki (2012), Discharge height of lightning narrow bipolar events, *J. Geophys. Res.*, *117*, D05119, doi:10.1029/2011JD017054.

Wu, T., Y. Takayanagi, S. Yoshida, T. Funaki, T. Ushio, and Z. Kawasaki (2013), Spatial relationship between lightning narrow bipolar events and parent thunderstorms as revealed by phased array radar, *Geophys. Res. Lett.*, *40*, 618–623, doi:10.1002/grl.50112.

Wu, T., S. Yoshida, T. Ushio, Z. Kawasaki, Y. Takayanagi, and D. Wang (2014), Large bipolar lightning discharge events in winter thunderstorms in Japan, *J. Geophys. Res. Atmos.*, *119*, 555–566, doi:10.1002/2013JD020369.